In: CIB-W18: Proceedings of 26th meeting; International council for building research studies and documentation working commission W18-Timber structures; 1993 August; Athens, GA. [Place of publication unknown]; [Publisher unknown]; 1994. 16 p.

Simulation Analysis of Norwegian Spruce Glued-Laminated Timber

by

Roland Hernandez and Robert H. Falk

Research Engineers
Engineered Wood Products and Structures

USDA Forest Service
Forest Products Laboratory[1]
One Gifford Pinchot Drive
Madison, WI USA 53705-2398

ABSTRACT

A computer analysis model, referred to as PROLAM, was used to simulate the performance of glued-laminated (glulam) timber beams manufactured from Norwegian spruce lumber. Mechanical properties of tested lumber and finger joints were analyzed to determine the input properties required by the model, and Monte Carlo simulation procedures were used to compile and characterize bending strength and stiffness distributions of the glulam beams. Simulated glulam beam results compared reasonably well with actual results. Sensitivity analyses were also conducted to observe both the effects of redistribution of stresses within a glulam beam, and the influence of finger-joint tensile strength on glulam beam bending strength.

INTRODUCTION

Recently, a large-scale research program was conducted at the Norwegian Institute of Wood Technology to study the performance of glued-laminated (glulam) timber manufactured from Norwegian spruce lumber (Falk et al. 1992). The laminating grades of Norwegian spruce involved in this research program were the C37-14E and C30-12E grades specified in the EN TC 124.203 Standard (Comite European de Normalisation 1990a). The glulam layups studied were the homogeneous LH35 and

[1]The Forest Products Laboratory is maintained in cooperation with the University of Wisconsin. This article was written and prepared by U.S. Government employees on official time, and it is therefore in the public domain and not subject to copyright.

LH40 as specified in the EN TC 124.207 Standard (Comite European de Normalisation 1990b) and a modified version of the LC38 combined layup. Extensive information was gathered on the laminating lumber and finger joints, which made it possible to analyze the glulam beams using procedures from both the European and American standards (Falk and Hernandez, In press). Information on strength, stiffness, density, and knot size for the lumber specimens was then used as input for advanced glulam simulation models such as those by Ehlbeck and Colling (1986), and by Hernandez et al. (1992). This paper deals with the simulation analysis of glulam beams manufactured from Norwegian spruce lumber using the Hernandez et al. model, referred to as PROLAM.

Preliminary work was conducted to analyze the mechanical properties of the Norwegian spruce laminating lumber. This work included analyzing lumber and end-joint properties to characterize statistical distributions of strength and stiffness, as well as to determine the correlations between strength and stiffness. The specific information on the laminating lumber was used as input for the PROLAM model to simulate the performance of the glulam beams.

OBJECTIVES

The overall objective of this study was to verify that the PROLAM model can predict the performance of glulam beams of European manufacture. Specific objectives of this paper were to

(1) compare actual and simulated performance of glulam beams made from Norwegian spruce laminating stock, and

(2) conduct sensitivity analyses to observe the effects of varying manufacturing parameters.

BACKGROUND

The PROLAM model uses distributions of mechanical properties of laminating stock and finger joints to determine the mechanical properties of full-size glulam beams. In addition, the model considers within-piece correlation between the tensile strength of the lamination ($f_{t,lam}$) and the flatwise modulus of elasticity (MOE_{flat}). The sequence of events in the simulation of a single beam using PROLAM involves simulating the beam layup, assigning lamination and finger-joint properties, determining beam strength using a simple transformed section method, and determining beam stiffness using a complementary virtual work procedure. A detailed description of this simulation process is described in Hernandez et al. (1991). Prior to this study, modifications were made to the PROLAM model. One modification was simulating finger-joint tensile strength $f_{t,fj}$ from statistical distributions fitted to actual test data, rather than from a regression relationship between finger-joint stiffness and $f_{t,fj}$. A

second modification was the implementation of a method to consider the interaction of tensile and bending stresses in the laminations of shallow glulam beams.

PROCEDURES

In this study, a detailed analysis was conducted on the laminating lumber properties described by Falk et al. (1992). The following sections describe the characterization of input required by the PROLAM model.

Characterizing lumber and finger-joint properties

In PROLAM, lumber length is simulated by entering a range and mode of length and a triangular distribution function to generate the values. In Falk et al. (1992), a relative frequency histogram of laminating lumber length used in the manufacture of the Norwegian spruce glulam beams was reported. The required distribution parameters for PROLAM were approximated from this histogram. The range of lumber length was approximately 2.2 to 5.6 m (7.2 to 18.4 ft) and the mode value of lumber length was approximately 4.5 m (14.8 ft). These parameters were used in PROLAM to generate lumber length for both the C37-14E and C30-12E grades.

MOE_{flat} properties were characterized using results of static tests conducted to verify machine stress grader output MOE_{mac}. These static tests were conducted across a 91.4-cm (36-in.) span on the full-length lumber specimens using a simply supported, center-point loading configuration (same configuration as the machine stress grader), Also, the location of the static test along the board length was selected such that a maximum visual defect existed between the supports. Appendix AI lists the statistical summaries of MOE_{flat} for both the C37-14E and C30-12E grades.

In addition to MOE_{flat} properties, PROLAM also requires a ratio between the MOE and modulus of rigidity to analyze beam stiffness. The ratios used for the C37-14E and C30-12E grades were determined from the EN TC 124.203 Standard, which specifies design levels for both “MOE Mean Parallel” and “Shear Modulus Mean”. The determined MOE to shear modulus ratios for C37-14E and C30-12E are 17.5 and 16.0, respectively. No adjustments were made to the calculated MOE_{flat} properties to adjust to a shear-free value because the estimated adjustment would have been less than 3 percent.

As explained in Falk et al. (1992), groups of C37-14E and C30-12E lumber were sorted for subsequent ultimate tensile strength ($f_{t,lam}$) testing. This testing was conducted specifically for the requirements of the PROLAM model, that is, with a 61-cm (24-in.) span between the grips. Two tension specimens were cut from each board. The tensile strength values were from a matched group of lumber not reported in Falk et al. (1992). The reported tension tests were tested across a 1-m (39-in.) span and had a maximum visual defect located between the tension grips. The lumber tested for PROLAM input was not biased with respect to selection based on

visual defects. Appendix A2 shows the statistical summaries of the 61-cm (24-in.) $f_{t,lam}$ properties compared with the 1-m (39-in.) span $f_{t,lam}$ properties reported in Falk et al. The $f_{t,lam}$ values tested at 61 cm (24 in.) were 8 and 11 percent higher at the 50th percentile level than were the f_t results tested at a 1-m (39-in.) span for the C37-14E and C30-12E grades, respectively; at the 5th percentile level, this difference was 19 and 26 percent higher, respectively. The 5th percentile difference can probably be attributed to a combination of length effect in tension testing and also to the fact that the 1-m (39-in.) tests were conducted with a maximum visual defect within the test span.

In addition to solid lumber, Falk et al. (1992) also tested finger joints from the C37-14E and C30-12E grades that were manufactured during the same production run as the manufacture of the full-size glulam beams. The ultimate finger-joint tensile strength $f_{t,lam}$ was determined across a 30-cm (12-in.) span. This test span was chosen so that the majority of the failures occurred at the finger-joint location. Appendix A3 summarizes the $f_{t,fj}$ properties for both the C37-14E and C30-12E laminating grades.

Determining correlation between lumber properties

To simulate localized laminating properties with PROLAM, a model developed by Taylor and Bender (1991) was used that considers the lengthwise correlation of the segmented values of MOE_{flat} and of $f_{t,lam}$ along a piece of laminating lumber, as well as the correlation between these two properties. This lengthwise correlation of one property is referred to as serial correlation, and the correlation between properties is referred to as cross correlation. Also, the correlation between segments is referred to as lag correlation. For example, correlations between the four segments marked on the tested lumber specimens were related such that segment 1 and segment 2 had a lag-1 correlation, segment 1 and segment 3 had a lag-2 correlation, and segment 1 and segment 4 had a lag-3 correlation. To establish these correlations from actual lumber properties, MOE_{flat} and $f_{t,lam}$ data on adjacent 61-cm (24-in.) lumber segments are needed.

For this study, however, MOE_{flat} properties were not obtained on adjacent segments. Therefore, the serial correlation of MOE_{flat} was estimated from the MOE_{mac} properties. Estimates of the lag-1, lag-2, and lag-3 serial correlations of MOE_{mac} were determined on 1,460 specimens of C37-14E lumber and 1,483 specimens of C30-12E lumber.

Serial correlation for $f_{t,lam}$ was determined from the results of tested lumber. Because segments 1 and 4 were tested in tension, lag-3 serial correlation of $f_{t,lam}$ was determined from the test results. Lag-1 and lag-2 values were estimated. To determine the serial correlation for $f_{t,lam}$, 93 specimens were used for the C37-14E grade and 100 specimens were used for the C30-12E grade.

Cross correlation between MOE_{mac} and $f_{t,lam}$ was determined from the same test group used for determining serial correlation of $f_{t,lam}$. Appendix A4 shows the estimates of

the lag-0 through lag-3 serial and cross correlations of MOE_{mac} and $f_{t,lam}$ for the C37-14E and C30-12E laminating grades, as well as for both grades combined.

When all data were combined, the estimated serial and cross correlations for MOE_{mac} and $f_{t,lam}$ increased. A possible explanation for this increase is that when data were combined, a larger range of properties were being analyzed and trends in the within-piece correlations of MOE_{mac} and $f_{t,lam}$ were better detected.

Comparing actual and simulated glulam beam properties

The three combinations of glulam that were studied in Falk et al. (1992) were the homogeneous LH35 and LH40 layups and the combination LC38* layup (Fig. 1). The LC38 layup was modified to LC38* because C30-12E lumber grade was used in the core laminations instead of the specified C24-12E grade. The lumber properties previously discussed for the C37-14E and C30-12E grades were used as input in the PROLAM model, along with the dimensions, layup, and loading configuration of the actual glulam beams.

The glulam beam results were analyzed by comparing cumulative distribution functions (CDF) and/or statistical summaries of the actual and simulated bending strength and stiffness. Bending strength refers to modulus of rupture (MOR) and bending stiffness refers to MOE. Simulation results of 1,000 beams of each glulam beam combination were compiled to construct the CDFs. In addition, 10 independent batches of 104, 96, and 112 beams (actual sample sizes of each tested beam group) were simulated for the LH35, LC38*, and LH40 layups, respectively, to construct 90 percent confidence intervals (at 75 percent tolerance) on each property. Figures 2 through 4 compare TEST and SIMULATED glulam MOR for the LH35, LC38*, and LH40 layups, respectively. Table 1 lists the statistical summaries of the TEST and SIMULATED results for both glulam MOR and MOE.

Figures 2 through 4 indicate that both the TEST and SIMULATED glulam beam bending strengths have nearly equal MOR properties at the 5th percentile levels. Table 1 shows that TEST results were not bounded well by the confidence intervals constructed on the SIMULATED results for all properties and beam layups at the 50th percentile level. At the 5th percentile levels, TEST results were bounded (or nearly so) by the confidence intervals constructed on the SIMULATED results. The differences between TEST and SIMULATED glulam MOR results were 10, 5, and 11 percent at the 50th percentile and 2, 6, and 3 percent at the 5th percentile for the LH35, LC38*, and LH40 layups, respectively. It appears that glulam MOR at the lower percentiles was predicted to within 6-percent of the TEST results. However, results at the upper percentiles were within 11 percent. Also, differences between TEST and SIMULATED glulam MOE at both the 50th and 5th percentiles were within 4 percent for the LC38* and LH40 layups, and within 10 percent for the LH35 layup.

It is speculated that part of the rather large difference in TEST and SIMULATED MOE results of the LH35 layup compared with the other layups could be attributed to the possibility that the input MOE_{flat} properties for the C30-12E grade were somewhat low. For example, Appendix Al shows an average MOE_{flat} value of 13.9 GPa ($2.02x10^6$ Ib/in^2) for the C37-14E grade; correspondingly, Table 1 shows a 50th percentile glulam MOE value of 14.1 GPa ($2.05x10^6$ Ib/in^2) for the LH40 layup. Because the C37-14E grade is less likely to have large stiffness-reducing knots, it is logical that only a 1.4-percent difference was observed between the MOE_{flat} properties of the C37-14E grade and the MOE properties of a homogeneous glulam beam made from the same grade. On the other hand, the average MOE_{flat} value for the C30-12E grade in Appendix A1 is 11.2 GPa ($1.63x10^6$ Ib/in^2) and Table 1 shows a 50th percentile glulam MOE value of 12.1 GPa ($1.76x10^6$ Ib/in^2) for the LH35 layup. The difference between MOE_{flat} and glulam beam MOE for the C30-12E grade was 7.4 percent. Because the lower quality C30-12E grade likely possesses larger stiffness-reducing knots, compounded with the fact that these maximum visual defects were purposely placed in the test span, it is suspected that the MOE_{flat} estimates for this grade are somewhat low.

In addition to influencing the SIMULATED glulam beam MOE, the MOE_{flat} properties of the lumber also influenced the SIMULATED beam MOR through the distribution of stresses in the transformed section analysis. For example, Table 1 shows that the lower 5th percentile of the TEST glulam MOR of the LC38* layup were not bounded by the confidence interval of the SIMULATED results. However, because the LC38* layup consists of C30-12E core laminations, it is possible that the lower MOE_{flat} properties in these core laminations caused a greater amount of stress to be distributed to the outer C37-14E laminations; this may have caused the simulated beams to reach failure criteria prematurely. This redistribution of stresses is the topic of the first sensitivity analysis in the next section.

Sensitivity analyses

Redistribution of stresses

The effect of redistribution of stresses from lower stiffness to higher stiffness laminations was studied in this sensitivity analysis. Simulations dealt with a homogeneous 9-lamination beam that had an MOE_{flat} distribution with an average of 13.8 GPa ($2.00x10^6$ Ib/in^2) and a coefficient of variation (COV) of 10 percent. Although this layup was not the same as that for the LH40 beams, the same size and loading configurations as those for the g-lamination beams studied earlier were used. The input $f_{t,lam}$ distribution was determined using the MOE/$f_{t,lam}$ regression relationship established by Falk et al. (1992). To observe the effect of redistributed stresses on glulam beam bending strength, the MOE_{flat} of the single top and bottom laminations were kept constant and mean values of MOE_{flat} of the inner seven laminations were reduced by 5 percent for each subsequent simulation run (13.1 GPa, 12.4 GPa, etc.) to a value of 10.3 GPa ($1.49x10^6$ Ib/in^2). The COV of each MOE_{flat} distribution was held constant at 10 percent, and the $f_{t,lam}$ distribution was held constant at a level

corresponding to a 13.8-GPa MOE_{flat} distribution. Finger-joint tensile strength was excluded from this analysis. This scaling of the MOE_{flat} distribution while holding the $f_{t,lam}$ constant allowed us to directly observe the effect of redistributing stresses from lower to higher stiffness laminations on glulam beam strength. Scaling the MOE_{flat} and holding the $f_{t,lam}$ constant did not simulate the behavior of actual beams, because lower stiffness lumber generally would have lower tensile strengths. For this reason, a second simulation analysis was conducted where in addition to scaling the MOE_{flat} properties, the corresponding $f_{t,lam}$ properties were determined from the same MOE-$f_{t,lam}$ regression relationship for each new level of MOE_{flat}. Thus, the first case scenario showed the effect of redistribution of stresses, solely caused by changing lamination stiffness. The second case scenario simulated the same phenomenon; however, decreasing $f_{t,lam}$ was considered.

Figure 5 illustrates the results of varying the MOE_{flat} values of the core laminations. In Figure 5, the difference between the MOE_{flat} values of the single outer lamination (OUTER) and the MOE_{flat} of the remaining core laminations (CORE) was varied from a 0-percent difference between OUTER and CORE to a 25-percent difference between OUTER and CORE. Figure 5 illustrates that even with a OUTER/CORE difference in MOE_{flat} as high as 25 percent, the 5th percentile of glulam MOR, referred to as $MOR_{.05}$, dropped only 3.4 percent when compared to the homogeneous layup with the $f_{t,lam}$ held constant. However, when the $f_{t,lam}$ distribution was determined for each corresponding level of MOE_{flat}, the $MOR_{.05}$ results dropped by 15.3 percent when the OUTER/CORE MOE_{flat} difference was 25 percent.

This result implies that for nonhomogeneous glulam layups, if the decrease in strength at the 5th-percentile level $MOR_{.05}$ was arbitrarily limited to 10 percent, then the OUTER/CORE MOE_{flat} difference should be no larger than 15 percent. This applies to beams with 10 percent higher quality material on the top and bottom laminations. These results also indicated that SIMULATED glulam MOE decreased by 5 percent when the core lamination MOE_{flat} values were decreased by 10 percent. When the MOE_{flat} value of the core was decreased by 25 percent, the glulam beam MOE decreased by 14 percent.

Finger-joint tensile strength

Another parameter studied was the influence of finger-joint tensile strength $f_{t,fj}$ on glulam beam performance. In PROLAM, an option is provided that allows the user to bypass the influence of $f_{t,fj}$ when determining the maximum moment carrying capacity of the glulam beams. Table 2 shows simulated results without the influence of finger joints (referred to as No FJ) for both the 50th and 5th percentiles of MOR, $MOR_{.50}$ and $MOR_{.05}$ respectively. Also in Table 2, ratios between simulated results without finger joints and with finger joints were compared. At both percentile levels of MOR, bending strength values were within 4 percent for all three beam layups when compared with the SIMULATED results of Table 1. In Falk et al. (1992), the ratio between ACTUAL mean glulam beam bending strength for all beams and those beams that failed only in the lamination was 0.99, 0.98, and 1.02 for the LH35, LC38*, and

LH40 layups, respectively. Thus, both the No FJ and SIMULATED results indicate that the tensile strength of the finger joints had little influence on the overall bending strength performance of the shallow glulam beams evaluated in this study. This observation, however, is not typical of all glulam beam tests.

CONCLUSION

In summary, the lumber and finger-joint data from Falk et al. (1992) were analyzed to develop input properties required by a glulam beam simulation model developed by Hernandez et al. (1991). When the input lamination property values were used to simulate glulam beam performance, SIMULATED results compared well with the TEST results.

Sensitivity analyses indicated that when the tensile strength of all the laminations were held constant and only the CORE laminations were reduced in stiffness, the decrease in bending strength was less than 4 percent. However, when the same stiffness configurations were modeled while considering the reduction in lamination tensile strength corresponding to the reduced stiffness of the core laminations, the reduction in glulam bending strength was approximately 15 percent. This implies that the difference between OUTER and CORE lamination stiffness be kept to a minimum of 15 percent to minimize the reduction in glulam bending strength to within 10 percent.

The second sensitivity analysis involved studying the influence of finger-joint tensile strength on the performance of the glulam beams in this study. Comparing simulated results without the influence of finger joints to simulated results with the influence of finger joints were only within 4 percent at both the 50th and 5th percentiles of glulam MOR. This suggested that for the glulam layups evaluated in this study, finger joints played a marginal role in the overall bending strength performance of the beams. This observation was supported by the actual results of the tested glulam combinations.

REFERENCES

Comite European de Normalisation. 1990a. Draft Standard EN TC 124.203, Structural Timber - Strength Classes.

Comite European de Normalisation. 1990b. Draft Standard EN TC 124.207, Glued-Laminated Timber - Strength Classes and Determination of Characteristic Properties.

Ehlbeck, J. and F. Colling. 1986. Strength of Glued Laminated Timber, CIB W18/19-12-1.

Falk, R.H. and R. Hernandez. In press. The Performance of Glued-Laminated Beams of European Manufacture.

Falk, R.H., K.H. Solli, and E. Aasheim. 1992. The Performance of Glued-Laminated Timber Beams Manufactured from Machine Stress Graded Norwegian Spruce, Report No. 77, Norwegian Institute of Wood Technology, Oslo.

Hernandez, R., D.A. Bender, B.A. Richburg, and K.S. Kline. 1992. Probabilistic Modeling of Glued-Laminated Timber Beams. Wood and Fiber Science, 24(3):294-306.

Taylor, S.E. and D.A. Bender. 1991. Stochastic Model for Localized Tensile Strength and Modulus of Elasticity in Lumber. Wood and Fiber Science, 23(4):501-519.

Table 1: TEST and SIMULATION results of glulam beam modulus of rupture (MOR) and modulus of elasticity (MOE)[a]

Glulam layup	Sample size	$MOR_{.50}$[b] (MPa)	$MOR_{.05}$[b] (MPa)	$MOE_{.50}$[b] (GPa)	$MOE_{.05}$[b] (GPa)
TEST results					
LH35	104	44.5	33.2	12.1	11.0
LC38*	96	47.8	39.2	13.4	12.4
LH40	112	52.6	39.9	14.1	12.8
SIMULATED results					
LH35	1040	40.6 (39.4, 41.9)	32.4 (30.1, 34.6)	11.0 (10.9, 11.1)	10.3 (10.1, 10.4)
LC38*	960	45.5 (43.4, 47.6)	36.9 (34.7, 39.1)	13.1 (12.9, 13.2)	12.5 (12.3, 12.6)
LH40	1120	47.6 (46.4, 48.91	38.6 (35.7, 41.5)	13.6 (13.4, 13.7)	12.9 (12.7, 13.1)
Ratio TEST/SIMULATED MOR					
LH35		1.10	1.02		
LC38*		1.05	1.06		
LH40		1.11	1.03		
Ratio TEST/SIMULATED MOE					
LH35				1.10	1.07
LC38*				1.02	0.99
LH40				1.04	0.99

[a] Statistics are based on nonparametric estimates.
[b] Values in parentheses are 90 percent confidence interval limits at 75 percent tolerance (lower, upper); 1 MPa = 145.0 lb/in^2, 1 GPa = 0.15x10^6 lb/in^2.

Table 2: Simulated glulam beam properties without the influence of finger-joint tensile strength[a]

Glulam layup	Sample size	$MOR_{.50}$[b] (MPa)	$MOR_{.05}$[b] (MPa)	Ratio No FJ/Simulated	
				$M0R_{.50}$	$MOR_{.50}$
No FJ[c]					
LH35	1040	41.8 (40.6, 43.0)	33.3 (30.7, 35.8)	1.03	1.03
LC38*	960	47.5 (45.4, 49.7)	38.4 (35.9, 40.9)	1.04	1.04
LH40	1120	49.6 (48.3, 50.9)	39.8 (37.3, 42.3)	1.04	1.03

[a] Statistics based on nonparametric estimates.
[b] Values in parentheses are 90 percent confidence interval limits at 75 percent tolerance (lower, upper).
[c] Simulated glulam beam results when finger joint tensile strength not considered in determination of ultimate moment carrying capacity of glulam beams.

Appendix A1 : Statistical summary of lumber MOE_{flat}

Lumber grade	Sample site	Average MOE_{flat} (GPa ($x10^6$ lb/in^2))	COV (%)
C37-14E	204	13.9 (2.016)	14.8
C30-12E	221	11.2 (1.628)	11.9

PROLAM input distribution parameters for MOE_{flat} ($x10^6$ lb/in^2)

Lumber grade	Distribution type	Location	Scale[a]	Shape[a]
C37-14E	LogNormal	0.6722	0.2848	0.1472
C30-12E	Weibull	0.4144	1.2935	7.4242

l For the lognormal distribution, Scale is mean of ln(X) and Shape is standard deviation of ln(X).

Appendix A2: Statistical summary of $f_{t,lam}$ and f_t[a]

Lumber grade	Sample size	Average (MPa ($x10^6$ lb/in^2))	COV (%)	5th percentile (MPa ($x10^6$ lb/in^2))
$f_{t,lam}$				
C37-14E	186	44.0 (6.380)	17.9	31.2 (4.530)
C30-12E	200	37.3 (5.410)	17.9	26.2 (3.800)
f_t[a]				
C37-14E	199	40.9 (5.940)	22.0	26.2 (3.790)
C30-12E	215	33.7 (4.880)	21.8	20.8 (3.010)

[a] f_t tested across a 1-m (39-in.) span from Falk et al. (1992). unadjusted for width.

PROLAM input distribution parameters for $f_{t,lam}$

Lumber grade	Distribution type	Location ($x10^3$ lb/in^2)	Scale ($x10^3$ lb/in^2)	Shape
C37-14E	Weibull	3.1058	3.6535	3.1441
C30-12E	Weibull	2.3033	3.4500	3.5602

Appendix A3: Statistical summary of $f_{t,fj}$

Lumber grade	Sample size	$f_{t,fj,mean}$ (MPa ($x10^3$ lb/in^2))	COV (%)	$f_{t,fj,.05}$ (MPa ($x10^3$ lb/in^2))
C37-14E	100	37.7 (5.470)	14.7	27.9 (4.050)
C30-12E	99	33.8 (4.910)	14.9	25.7 (3.720)

PROLAM input distribution parameters for $f_{t,fj}$

Lumber grade	Distribution type	Location ($x10^3$ lb/in^2)	Scale ($x10^3$ lb/in^2)	Shape
C37-14E	Weibull	1.6081	4.1806	5.5364
C30-12E	Weibull	2.8174	2.3338	3.1389

Appendix A4: Summary of estimated serial and cross correlations for MOE_{mac} and $f_{t,lam}$

C37-14E	Serial MOE_{mac}	Serial $f_{t,lam}$	Cross MOE-$f_{t,lam}$
lag-0	1.0000	1.0000	0.3340
lag- 1	0.7096	0.6888	0.2370
lag-2	0.5632	0.4744	0.1881
lag-3	0.3572	0.3268	0.1193

C30-12E	Serial MOE_{mac}	Serial $f_{t,lam}$	Cross MOE-$f_{t,lam}$
lag-0	1.0000	1.0000	0.3685
lag-I	0.6679	0.5653	0.2461
lag-2	0.4270	0.3195	0.1573
lag-3	0.2980	0.1806	0.1098

C37-C30 Combined	Serial MOE_{mac}	Serial $f_{t,lam}$	Cross MOE-$f_{t,lam}$
lag-0	1.0000	1.0000	0.5372
lag-1	0.8720	0.6448	0.4684
lag-2	0.7604	0.4158	0.4085
lag-3	0.6631	0.2681	0.3562

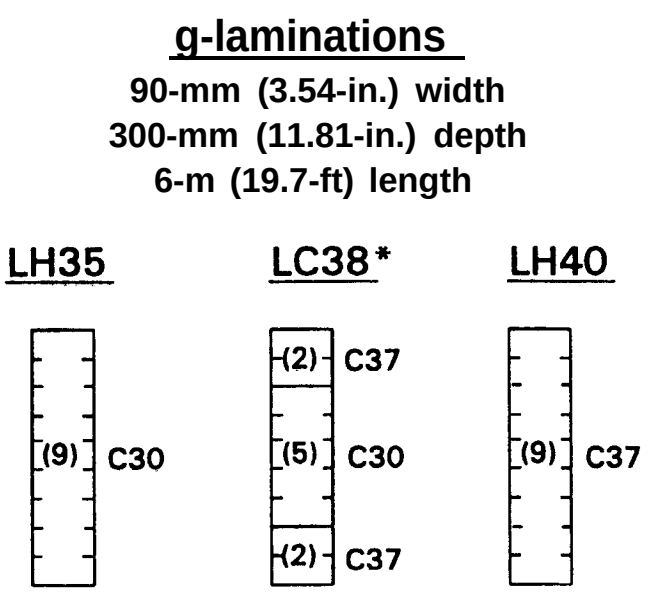

Figure 1: Norwegian spruce glulam layups showing placement of laminating lumber grades.

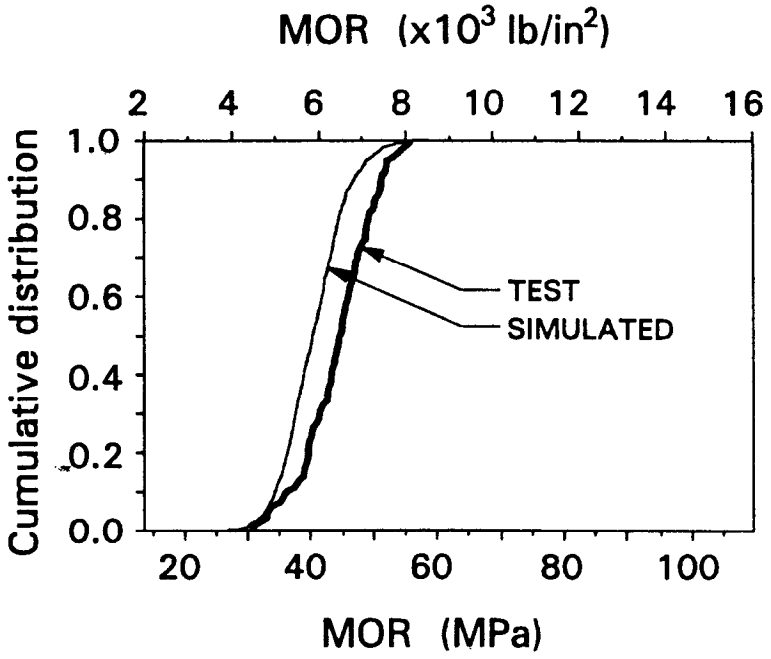

Figure 2: Empirical cumulative distribution functions of TEST and SIMULATED MOR for LH35 Norwegian spruce glulam beam layup.

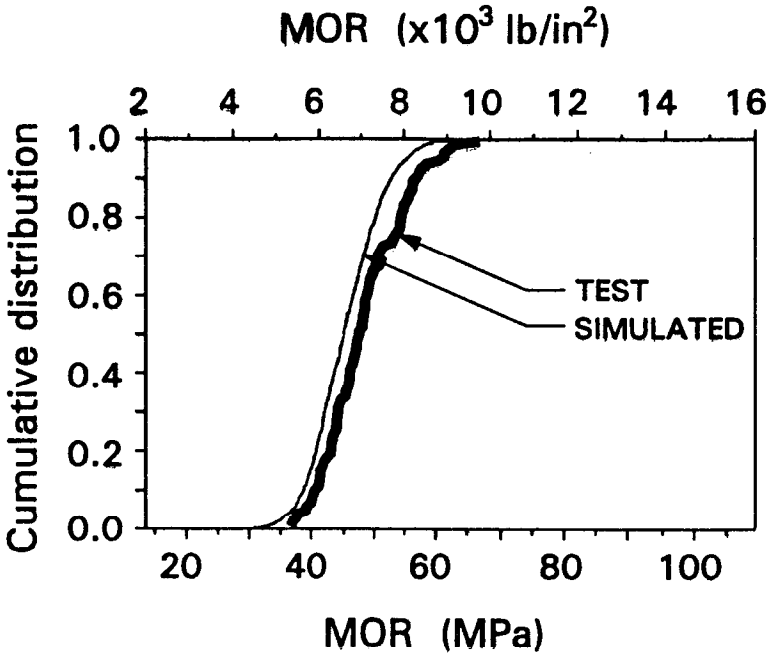

Figure 3: **Empirical cumulative distribution functions of TEST and SIMULATED MOR for LC38* Norwegian spruce glulam beam layup.**

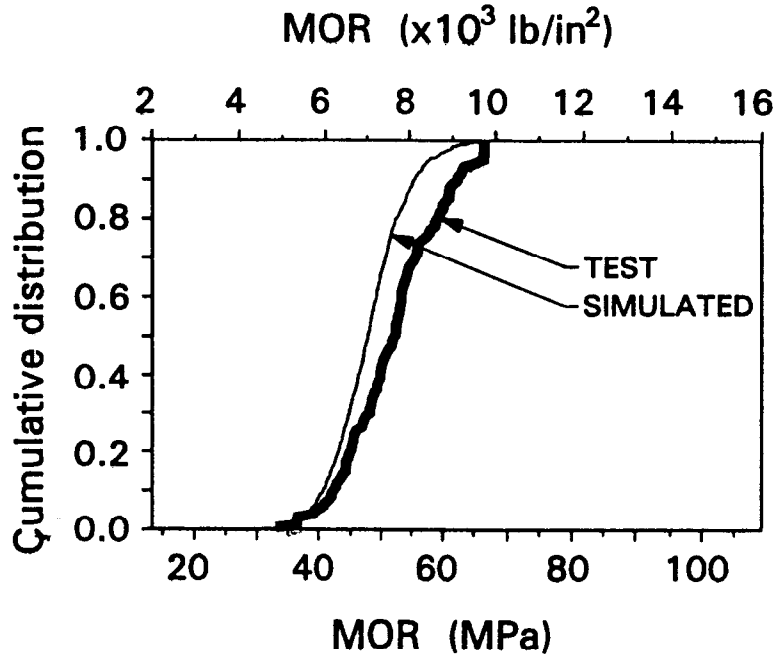

Figure 4: **Empirical cumulative distribution functions of TEST and SIMULATED MOR for LH40 Norwegian spruce glulam beam layup.**

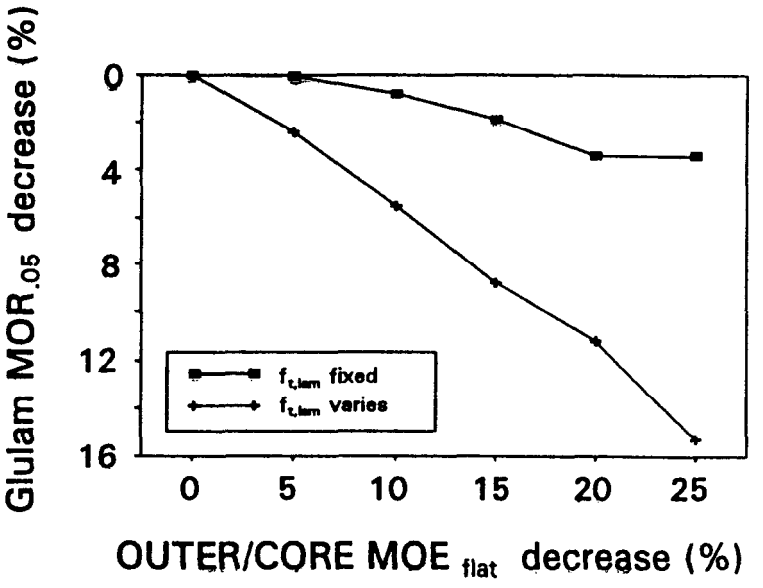

Figure 5: **Graph showing change in glulam $MOR_{.05}$ as OUTER to CORE lamination MOE_{flat} changes.**